

The Early Metazoan *Trichoplax adhaerens* Possesses a Functional O-GlcNAc System^{*[5]}

Received for publication, December 1, 2014, and in revised form, March 9, 2015 Published, JBC Papers in Press, March 16, 2015, DOI 10.1074/jbc.M114.628750

Nithya Selvan[‡], Daniel Mariappa[§], Henk W. P. van den Toorn[¶], Albert J. R. Heck[¶], Andrew T. Ferenbach[‡], and Daan M. F. van Aalten^{‡§1}

From the [‡]Division of Molecular Microbiology and [§]MRC Protein Phosphorylation and Ubiquitylation Unit, College of Life Sciences, University of Dundee, Dow Street, Dundee, DD1 5EH, United Kingdom and the [¶]Biomolecular Mass Spectrometry and Proteomics, Bijvoet Center for Biomolecular Research and Utrecht Institute for Pharmaceutical Sciences, Utrecht University, Padualaan 8, 3584 CH Utrecht, The Netherlands

Background: Protein O-GlcNAcylation and orthologues of O-GlcNAc transferase (OGT) and O-GlcNAcase (OGA) occur separately or together in all kingdoms of life.

Results: The basal metazoan *Trichoplax adhaerens* is the simplest organism to possess functional OGT, OGA, and protein O-GlcNAcylation together.

Conclusion: Reversible protein O-GlcNAcylation is conserved throughout the metazoan lineage.

Significance: *T. adhaerens* can be used as a reductionist model to identify evolutionarily conserved O-GlcNAc targets.

Protein O-GlcNAcylation is a reversible post-translational signaling modification of nucleocytoplasmic proteins that is essential for embryonic development in bilateria. In a search for a reductionist model to study O-GlcNAc signaling, we discovered the presence of functional O-GlcNAc transferase (OGT), O-GlcNAcase (OGA), and nucleocytoplasmic protein O-GlcNAcylation in the most basal extant animal, the placozoan *Trichoplax adhaerens*. We show via enzymatic characterization of *Trichoplax* OGT/OGA and genetic rescue experiments in *Drosophila melanogaster* that these proteins possess activities/functions similar to their bilaterian counterparts. The acquisition of O-GlcNAc signaling by metazoa may have facilitated the rapid and complex signaling mechanisms required for the evolution of multicellular organisms.

Post-translational protein O-GlcNAcylation is the reversible addition of β -D-N-acetylglucosamine (GlcNAc) to serine and threonine residues on metazoan nucleocytoplasmic proteins (1). O-GlcNAc transferase (OGT)² and O-GlcNAcase (OGA) are the enzymes responsible for the addition and removal of O-GlcNAc, respectively. Since it was first described in 1984 (2), O-GlcNAc has become associated with a range of cellular processes (1). There appears to be extensive cross-talk between O-GlcNAc and Ser/Thr phosphorylation, with the two modifications occurring at the same or neighboring residues on pro-

teins (3–5). O-GlcNAcylation of several kinases (AMP-activated protein kinase, CaMKIV, and CaMKII, for example) regulates their activity, and OGT functionally interacts with two catalytic subunits of protein phosphatase 1 (6–9). The discovery of O-GlcNAc on proteasome subunits in *Drosophila* implicates a role for this post-translational modification in protein trafficking and degradation (10). O-GlcNAcylation increases in the presence of stressors like heat and heavy metals (11, 12), and protects cardiac tissues following ischemia (13). Reports have emerged of the involvement of O-GlcNAc in gene expression and epigenetics. The discovery of O-GlcNAc on RNA polymerase II transcription factors suggested a role for the modification in transcriptional activation (14). Overexpressing OGT in mitotic cells was shown to alter methylation and phosphorylation of histone H3 (15). In addition, cell cycle-dependent O-GlcNAc cycling was also found to occur on histones H2A, H2B, and H4 (16). Transcriptional repression by OGT involving interactions with mSin3A and HDAC1 has been demonstrated (17). Activation of gene expression downstream of H2B O-GlcNAcylation has been characterized, as well as transcriptional changes due to H3K4 trimethylation facilitated by the TET protein-OGT complex (18, 19). O-GlcNAcylation is associated with disease conditions like Type II diabetes, Alzheimer disease, and cancer (1, 20).

Following the identification of OGT and OGA activities (21–23) and their enzymatic characterization (23, 24), transcripts have been cloned from humans and other organisms (25, 26) and found to be highly conserved in animals. In humans, a single *OGT* gene encodes three isoforms of the protein, the longest, nucleocytoplasmic OGT (ncOGT/hOGT), is a ~116 kDa protein and possesses 13.5 tetratricopeptide repeats (TPRs) at its N terminus (27, 28). Another isoform possessing 9.5 TPRs and a mitochondrial localization signal (mOGT ~103 kDa) is targeted to mitochondria. The shortest OGT isoform (sOGT ~78 kDa) contains only 2.5 TPRs and also has nucleocytoplasmic localization (27). In *Drosophila* and *Caenorhabditis elegans*, single *ogt* genes encode a single protein similar to

^{*} This work was supported by Wellcome Trust Senior Research Fellowship WT087590MA (to D. M. F. v. A.).

✂ Author's Choice—Final version free via Creative Commons CC-BY license.

[5] This article contains supplemental Figs. S1 and S2.

The nucleotide sequence(s) reported in this paper has been submitted to the DDBJ/GenBank™/EBI Data Bank with accession number(s) KP663422, KP663423, and KP663424.

¹ To whom correspondence should be addressed. Tel.: 00441382384979; Fax: 00441382388216; E-mail: dmfvanaalten@dundee.ac.uk.

² The abbreviations used are: OGT, O-GlcNAc transferase; OGA, O-GlcNAcase; TPR, tetratricopeptide repeat; HAT, histone acetyltransferase; 4MU-NAG, 4-methylumbelliferyl-N-acetyl- β -D-glucosaminide; PNGase F, peptide N-glycosidase F.

human ncOGT (27, 29–31). Zebrafish is exceptional among animals to possess two *ogt* genes encoding six variants of the protein at different stages of development (32).

In humans, a single gene encodes two isoforms of OGA. The longer cytoplasmic isoform (hOGA ~ 130 kDa) possesses an N-terminal catalytic domain and a C-terminal histone acetyltransferase (HAT)-like domain, whereas the shorter nuclear and lipid-droplet targeted isoform (~75 kDa) lacks the HAT-like domain (33, 34). In *C. elegans*, a single *oga* gene encodes four major transcripts generated by alternative splicing and in-frame intron utilization to produce proteins of different lengths containing both the catalytic and HAT-like domains (35). *Drosophila* has a single *oga* gene encoding a single protein. Toleman *et al.* (36) demonstrated HAT activity for hOGA purified from mammalian cells, which was, however, not observed in a subsequent study (37). Structural characterizations of putative bacterial acetyltransferases sharing sequence conservation with the HAT-like domain of hOGA enforce that hOGA lacks HAT activity (38, 39). Furthermore, the bacterially expressed hOGA HAT-like domain does not bind acetyl-CoA *in vitro* (38).

Although strides have been made toward identifying the processes regulated by O-GlcNAcylation, uncovering the consequences of O-GlcNAc on individual proteins at an organismal level remains a challenge. Gene knock-out is a useful strategy to addressing the challenge by generating animals lacking OGT/OGA activity. However, the fact that *Ogt* null mice and *Drosophila ogt* mutants die at different stages of development and *Oga* null mice as neonates (30, 40, 41) limits their use for functional studies. Whereas levels of OGT and OGA have been manipulated in zebrafish embryos and *Xenopus laevis* oocytes to study the roles of O-GlcNAc in development (42, 43), knock-outs of the enzymes have not been reported in these organisms. *C. elegans* is the only known example of an organism that remains viable and fertile after loss of OGT and OGA activity (29, 35). *ogt* and *oga* null mutants of *C. elegans* have therefore been used to study the effects of O-GlcNAc cycling on lifespan and aging (44–46). Accessible reductionist models with smaller O-GlcNAc proteomes are thus invaluable toward accelerating research into understanding the conserved roles and mechanisms of protein O-GlcNAcylation. The aim of this study was to find another such model.

Here, we report that the basal metazoan *Trichoplax adhaerens* is the simplest organism to possess both OGT and OGA and O-GlcNAcylated proteins. OGT appears to be expressed throughout the body of *Trichoplax* under basal conditions. *Trichoplax* OGT can rescue pupal lethality of the *Drosophila sxc* (*ogt*) mutant in addition to compensating for the maternal requirement of OGT. *Trichoplax* OGA can de-O-GlcNAcylate human and *Drosophila* cell lysates. Together, these data imply that the acquisition of OGA by metazoa at the time of diverging from their unicellular ancestors facilitated the cycling of O-GlcNAc on proteins. This acquisition may have expanded the repertoire of complex signaling mechanisms required for metazoan-specific features absent in other intracellular OGT-possessing organisms lacking OGA.

EXPERIMENTAL PROCEDURES

Sequences and Alignments—Orthologues of OGA and OGT in *Trichoplax* were identified by using BLAST in the Uniprot database and the *Trichoplax* genome database. Query sequences were from the following: *Homo sapiens*, *Mus musculus*, *Danio rerio*, *Drosophila melanogaster*, and *C. elegans*. Sequences were aligned using CLUSTALW, and edited and annotated with ALINE. XtalPred and sequence alignments with OgOGA were used to predict regions of structural disorder in hOGA, DmOGA and the TaOGAs. Surface views of hOGT and OgOGA were generated and colored by similarity to their *Trichoplax* counterparts using PyMOL.

T. adhaerens Culture and Harvest—Starter cultures of *T. adhaerens* and the cryptomonad marine red alga *Rhodomonas salina*, which serves as a food source for *Trichoplax*, were obtained from Prof. Leo Buss (Yale University). *Trichoplax* were seeded and grown on a mat of monoculture of *Rhodomonas* in 150-mm glass Petri dishes at 22 °C in artificial seawater (Reef Crystals, Aquarium Systems) of 36 parts per thousand (4.5 brx %) salinity supplemented with 0.1% (v/v) Micro Algae Grow (Florida Aqua Farms). To harvest *Trichoplax*, culture medium in Petri dishes was gently pipetted up and down several times to lift adherent animals off the glass surface. The contents of the dish were then centrifuged at 1000 × *g* at 4 °C for 10 min. The algae were removed by washing with unsupplemented artificial seawater by repeated centrifugation at low speed.

Rapid Amplification of cDNA Ends (RACE)—*Trichoplax* total RNA was extracted using TRI reagent (Sigma). cDNA was synthesized using Precision qScriptTM Reverse Transcription kit (Primer Design) and an oligo(dT) primer or the FirstChoice[®] RLM-RACE Kit (Ambion). Full-length coding sequences for *Trichoplax* OGA and OGT were determined using the FirstChoice[®] RLM-RACE Kit (Ambion) according to the manufacturer's instructions. PCR products were gel purified and sequenced. Full-length sequences were then amplified from cDNA and cloned into pCR[®]-Blunt II-TOPO[®] (Invitrogen) for sequence verification. Two to four colonies were sequenced using both the M13-F and M13-R primers.

Cloning and Site-directed Mutagenesis—TaOGA53 and TaOGA54 were cloned into pGEX6P1 and pOPTH, respectively, using a previously described restriction-free method (47) from TOPO clones after RACE experiments identified start and end sites. N-terminally truncated TaOGT was initially cloned through PCR amplification followed by BamHI-Sall digestion and ligation into pGEX6P1. Following identification of the start of TaOGT through RACE experiments, a missing segment was added to the existing construct by the restriction free cloning method. Site-directed mutations were introduced using the Stratagene QuikChange Site-directed mutagenesis kit except KOD Polymerase (Novagen) was used instead of Pfu, and DpnI was purchased from Fermentas. The presence of the intended mutations was confirmed by DNA sequencing.

Protein Expression and Purification—Plasmids containing TaOGT and TaOGA53 were transformed into *Escherichia coli* ArcticExpress competent cells (Stratagene), whereas TaOGA54 and hCK2α were transformed into *E. coli* BL21(DE3) pLysS cells. Cells were grown overnight at 37 °C in

Luria-Bertani medium containing 50 $\mu\text{g/ml}$ of ampicillin (LB-Amp) and used at 10 ml/liter to inoculate 6 liters of fresh LB-Amp in the case of BL21(DE3) pLysS cells and 12 liters for ArcticExpress cells. BL21(DE3) pLysS cells were grown to an A_{600} of 0.6–0.8, transferred to 18 °C, and induced with 250 μM isopropyl 1-thio- β -D-galactopyranoside and harvested after 16 h. ArcticExpress cells were grown to an $A_{600} = 1.0$, transferred to 12 °C, and induced with 250 μM isopropyl 1-thio- β -D-galactopyranoside and harvested after 72 h by centrifugation for 30 min at 3500 rpm (4 °C). Cell pellets were resuspended in 10–20 ml/liter of 50 mM Tris, 250 mM NaCl, and 0.5 mM Tris(2-carboxyethyl)phosphine (lysis buffer) at pH 9.0 for TaOGT and hCK2 α and pH 7.5 for TaOGA53 and TaOGA54. Lysis buffers for TaOGT and TaOGA53 also contained 5% glycerol and 0.05% Nonidet P-40. All lysis buffers were supplemented with protease inhibitors (1 mM benzamidine, 0.2 mM PMSF, and 5 μM leupeptin), DNase and lysozyme prior to lysis. Cells were lysed using a continuous flow cell disrupter (Avestin, 3 passes at 20 kpsi) and the lysate was cleared by centrifugation (30 min, 15,000 rpm, 4 °C). Supernatants were collected and loaded onto 2 ml of glutathione-Sepharose (GE Healthcare Life Sciences) pre-equilibrated with lysis buffer. TaOGA54 was loaded on to 2 ml of IMAC Sepharose (GE Healthcare) charged with NiSO₄ and pre-equilibrated with lysis buffer. Loaded resins were each washed with 500 ml of lysis buffer or lysis buffer containing 30 mM imidazole in the case of IMAC resin. The ArcticExpress chaperones were removed from captured GST-tagged proteins by washing the resin with 1 \times TBS (25 mM Tris, pH 7.5, 150 mM NaCl) containing 10 mM ATP and 11 mM MgCl₂ (4 \times washes at 37 °C). GST-tagged proteins were eluted from resin by cleavage of the GST tag using GST-tagged PreScissionTM protease at 4 °C for 16 h. His₆-tagged TaOGA54 was eluted using lysis buffer containing 250 mM imidazole and dialyzed into 1 \times TBS containing 0.5 mM Tris(2-carboxyethyl)phosphine. TaOGA54 and hCK2 α were further purified by size exclusion chromatography using a Superdex 200, 26/60 column. All proteins were concentrated using spin concentrators and purity was assessed by SDS-PAGE followed by Coomassie R-250 staining. Point mutants of TaOGT, TaOGA53, and TaOGA54 were purified the same way as their wild type counterparts.

Steady-state Kinetics— K_m for UDP-GlcNAc of wild type and mutant TaOGT was determined as described previously (48). Briefly, 100 μl reactions contained 100 nM TaOGT in 50 mM Tris, pH 7.5, 0.1 mg/ml of BSA, 10 μM sodium dithionite, and 100 μM peptide (KKENSPAVTPVSTA) and varying amounts of UDP-GlcNAc. Reactions were carried out for 75 min at room temperature and stopped using 200 μl of 37.5 μM fluorophore (48–50) prepared in 50 mM HEPES, pH 7.5, 10 mM NaCl, and 50% (v/v) methanol. Fluorescence was measured using Gemini EM plate reader (Molecular Devices) with excitation and emission wavelengths of 485 and 530 nm, respectively. The IC₅₀ for Goblin 1 was determined using 13 μM UDP-GlcNAc, 100 μM peptide, and varying concentrations of the inhibitor. Steady-state kinetics of wild type and mutant TaOGA54 and TaOGA53 were determined as described (51) using 4-methylumbelliferyl-N-acetyl- β -D-glucosaminide (4MUNAG, Sigma). Reaction mixtures (100 μl) contained 2–100 nM enzyme in 1 \times TBS, 0.1 mg/ml of BSA, and varying amounts of

substrate in 1–2% dimethyl sulfoxide. Reactions were performed for 30–120 min at room temperature and stopped by the addition of 200 μl of glycine-NaOH, pH 10.3. Fluorescence of released 4-methylumbelliferone was measured using a Synergy 2 plate reader (Bio-Tek), with excitation and emission wavelengths of 360 and 460 nm, respectively. IC₅₀ values were measured at K_m with varying concentrations of inhibitors. All experiments were performed in triplicate and measurements were corrected for background emission from reactions containing no peptide (for OGT assays) or no enzyme (for OGA assays). For all assays performed, substrate turnover was under 10%. Non-linear regression curves were fitted with Prism (GraphPad).

In Vitro O-GlcNAcylation of hCK2 α —Reactions contained 0.25 μg of hCK2 α , 3.7 mM UDP-GlcNAc, and 2.5 μM of either hOGT/GST-hOGT (purified as described previously (52)) or TaOGT in a total volume of 10 μl of 10 mM Tris, pH 7.5, and 1 mM DTT and incubated at room temperature for 1.5 h. For subsequent TaOGA treatments, GST-hOGT was pulled out of the reactions using glutathione-Sepharose and residual hOGT activity was blocked using 5 mM UDP. Reactions were stopped by the addition of Laemmli buffer and proteins were separated by SDS-PAGE and analyzed by Western blotting as described below.

Drosophila Genetics and Adult Fly Lysates—The following stocks were used: w^{1118} , sxc^1/CyO , sxc^6/CyO , and $tub::GAL4/TM6$. Transgenic flies were generated by Rainbow Transgenic Flies Inc., CA, with the attP insertion site at 86F8. 5 anesthetized male adult flies were frozen on dry ice and homogenized in 50 μl of lysis buffer (50 mM Tris-HCl, pH 8.0, 150 mM NaCl, 1% Triton X-100, 1 μM GlcNAcstatin C, 5 mM sodium fluoride, 2 mM sodium orthovanadate, 1 mM benzamidine, 0.2 mM PMSF, 5 μM leupeptin, and 1 mM DTT), following which an equal volume of 3 \times SDS Laemmli buffer was added. Lysates were then boiled for 5 min at 95 °C, centrifuged at 16,000 $\times g$ for 10 min, and supernatants were collected. 30 μg of crude lysates were used for Western blots.

Cell Culture, Lysis, and Protein Extraction—HEK293 cells were maintained in DMEM (Invitrogen) supplemented with 10% FBS (Gibco) and antibiotics (Gibco) at 37 °C in a humidified atmosphere. *Drosophila* S2 cells were cultured in Schneider's medium supplemented L-glutamine, 10% FBS (Gibco), and antibiotics (Gibco) at 25 °C. HEK293, S2 cells, and *Trichoplax* were lysed in 10 mM Tris, pH 7.5, 150 mM NaCl, 1% Nonidet P-40 supplemented with protease inhibitors (1 mM benzamidine, 0.2 mM PMSF, and 5 μM leupeptin). Transfected S2 cells were lysed with 50 mM Tris-HCl, pH 8.0, 150 mM NaCl, 1% Triton, 1 μM GlcNAcstatin C, 1 mM sodium orthovanadate, 5 mM sodium fluoride, and protease inhibitors. Lysates were cleared by centrifugation. Bradford assay or a Pierce 660-nm protein assay was used to quantify cell lysates.

Transfections, RNAi, and Enzymatic Treatments of Lysates—S2 cell transfections were carried out by mixing FuGENE HD (Roche), DNA (2 μg) at a 3:2 ratio ($\mu\text{l}:\mu\text{g}$) in 100 μl of sterile water. The constructs used for transfections were pMT-GAL4, pUAS-*DmOGT*^{WT}-HA, pUAS-TaOGT^{WT}-HA, and pUAS-TaOGT^{K815M}-HA. The metallothionein promoter was induced with 1 mM CuSO₄ 24 h after transfection. RNAi was performed

48 h before DNA transfections by transfecting 4 μ g of double-stranded RNA directed against the 3' UTR of *Dm*OGT transcript. Double-stranded RNA was synthesized using a TranscriptAid T7 High Yield Transcription Kit (Thermo) according to the manufacturer's instructions from PCR products containing T7 (indicated in lowercase in the primer sequences) sites introduced by the following primers: forward, taatagactactatagggAAAACGTTTATAATGTCAAT and reverse, taatagactactatagggTTCTTATTATATATCGTATA.

20 μ g of lysates were subjected to all enzymatic treatments. PNGase F (New England Biolabs) treatment was performed as described by the manufacturer. CpNagJ (purified as described in Ref. 51, but with the GST tag left uncleaved at the N terminus) treatment was performed with 2–4 μ g of the enzyme at 37 °C for 1 h. TaOGA54 and TaOGA53 treatments were performed on lysates and *in vitro* O-GlcNAcylated hCK2 α with 5, 10, or 15 μ g of the enzymes for 4 h at room temperature. Labeling of lysates with GalT1 (Y289L) was performed according to the manufacturer's instructions (Invitrogen).

Western Blotting—Proteins were resolved in SDS-PAGE gels and blotted onto nitrocellulose or PVDF membranes. Polyclonal antibodies were generated by immunizing rabbits (Dundee Cell Products) with a pair of peptides from each protein (TaOGT, EYADHYSEKLAFLPNS and TRLRKLQDKIWQLRHKC; TaOGA53, HKYGRHSIHLINMARC and TEATKHSSDATDTVDSC; and TaOGA54, LYLSHLEARFDSSVPEK and CRFILEQLKAKGSYGAS) and affinity purified using a 1:1 mixture of the peptide antigens coupled to NHS-activated agarose (Thermo). The following antibodies were used: anti-O-GlcNAc CTD110.6 (1:500, Covance), anti-O-GlcNAc RL-2 (1:3,000, Abcam), anti-actin (1:5,000, Sigma), anti-OGT DM-17 (1:5,000, Sigma), anti-OGT H-300 (1:1,000, Santa Cruz), anti-HA (12CA5, 1:2,500) and anti-CK2 α (1:5,000, Cell Signaling), anti-TaOGT (1:5,000 of \sim 8 μ g/ml), anti-TaOGA53 (1:5,000 of \sim 60 μ g/ml), and anti-TaOGA54 (1:5,000 of \sim 8 μ g/ml). HRP-conjugated anti-mouse IgM and IgG, anti-rabbit IgG, and ExtrAvidin[®]-peroxidase were purchased from Sigma. Biotin-conjugated concanavalin A was also purchased from Sigma and used as per the manufacturer's instructions. Anti-mouse Alexa Fluor[®] 680 and anti-rabbit Alexa Fluor[®] 790 were purchased from Jackson ImmunoResearch. Secondary antibodies were used at dilutions of 1:10,000 or 1:20,000. Blots were developed using ECL or imaged using the Li-Cor Odyssey infrared imaging system (Li-Cor). Blots with *Trichoplax* lysates were stained with Coomassie R-250 or Ponceau S for total protein loading.

In Situ Hybridization—*Trichoplax* were fixed as described (53) with slight modifications. Briefly, the animals were fixed using Lavdovsky's fixative (20% formaldehyde, 4% glacial acetic acid, 32% of 10 \times PBS, and 44% ethanol (v/v) in deionized water), washed, and permeabilized using PBST (1 \times PBS containing 0.1% Tween 20). Dioxigenin-labeled probes were synthesized using TranscriptAid T7 High Yield Transcription Kit (Thermo) according to the manufacturer's instructions from PCR products containing T7 (indicated in lowercase in the primer sequences) sites introduced to the sense or antisense strands by primers: sense forward, taatagactactatagggCGCATGGAAATCTTTGTTT, sense reverse, TCTGCGTATT-

CCATTGGTGA; antisense forward, CGCCATGGAAATCTTTGTTT, antisense reverse, taatagactactatagggTCTGCGTATTCCATTGGTGA.

Prehybridization and hybridization were carried out in 2.5 \times SSC buffer containing 50% formamide, 5% dextran sulfate, and 0.1 mg/ml of yeast tRNA. Approximately 0.5 μ g of probes were used per 1 ml of hybridization buffer and hybridizations were carried out overnight for each probe based on length of the probe and GC content at the temperature determined by the following formula,

$$T_{\text{hyb}} = \text{Eff } T_m - 20 \quad (\text{Eq. 1})$$

where $\text{Eff } T_m = 81.5 + 16.6(\log M [\text{Na}^+]) + 0.41(\%G + C) - 0.72(\% \text{ formamide})$.

Samples were then washed at low stringency using 100 mM maleic acid-buffered saline at pH 7.5 containing 0.1% Tween 20 (MABT). High stringency washes were performed with hybridization buffer at 98% stringency at temperatures determined using the following formula.

$$\text{Wash stringency \%} = 100 - (1 \times (\text{Eff } T_m - \text{washtemp})) \quad (\text{Eq. 2})$$

Samples were again washed in MABT, blocked with blocking buffer (3% BSA in MABT), and incubated in a 1:2000 dilution (in blocking buffer) of alkaline phosphatase-conjugated antidigoxigenin Fab fragments (Roche Diagnostics) for 5 h at room temperature. Following washes with MABT and deionized water, the color reaction was carried out using the alkaline phosphatase substrate BM purple (Roche Diagnostics). Samples were then mounted on slides with Vectashield medium-set mountant (Vector Biolabs) and imaged using a Leica DM2000 microscope (Leica Microsystems).

RESULTS

Trichoplax Expresses Orthologues of Metazoan OGT and OGA—We aimed to identify basal organisms possessing both OGT and OGA genes in an attempt to identify a reductionist model to probe O-GlcNAc signaling and shed light on the evolution of reversible intracellular protein O-GlcNAcylation. Reports have suggested the presence of O-GlcNAcylated proteins in filamentous fungi (54), protists (55, 56), and bacteria (57, 58). Plants and primitive eukaryotes possessing apparent OGT orthologues and O-GlcNAcylated proteins appear to lack OGA (55, 56, 59), suggesting that O-GlcNAcylation is either irreversible in these organisms, or may be reversed by unidentified enzymes bearing no similarity to metazoan OGA. Conversely, in the bacteria in which O-GlcNAc has been found, bioinformatics searches did not identify OGT-like proteins. We parsed the CAZy database, which lists a number of other organisms ranging from archaea to man that possess enzymes of the glycosyltransferase family 41 (GT41) and the glycoside hydrolase family 84 (GH84) to which OGT and OGA, respectively, belong. Upon close examination, it is clear that of all these organisms, only metazoa possess clear orthologues of both OGT and OGA (bearing over 40% sequence identity to hOGT and hOGA) in their genomes. We then searched the genomes of basal metazoa and identified an OGT gene fragment and two

candidate OGA gene fragments in the recently sequenced genome of *T. adhaerens* (60), the sole member of phylum placozoa. *Trichoplax* is a free-living marine organism considered to be one of the most basal extant multicellular organisms existing at the boundary between unicellular eukaryotes and metazoa (60–62). It contains only six cell types organized in three cellular layers (61, 63). The presence of putative stem cells at the periphery of the body of *Trichoplax* has been hypothesized (53), but remains unconfirmed (63).

Upon identifying fragments of *ogt* and *oga* genes in *Trichoplax* using bioinformatics, we performed 5' and 3' RACE (rapid amplification of cDNA ends) to obtain full-length sequences of these genes. It emerged that *Trichoplax* OGT (*TaOGT*), apart from having the catalytic domain, contains 13.5 N-terminal TPR repeats and a putative bipartite nuclear localization signal like hOGT (64) (Fig. 1a, supplemental Fig. S1a). It shares 66 and 64% overall amino acid sequence identity with hOGT and *D. melanogaster* OGT (*DmOGT*), respectively (Fig. 1a, supplemental Fig. S1a). Its active site is conserved with that of hOGT (supplemental Fig. S1b), and contains the key lysine residue (Lys-815 in *TaOGT* and Lys-842 in hOGT—Fig. 1a, supplemental Fig. S1a), shown to be critical for the activity of hOGT (52). The most variable region is the intervening domain within the catalytic lobes of the enzyme, whereas the TPRs are the most conserved (supplemental Fig. S1a). Unlike other metazoa, which possess a single *oga* gene, the genome of *Trichoplax* encodes for two putative OGAs, *TaOGA53* and *TaOGA54* (after their Uniprot IDs B3SB53 and B3SB54). *TaOGA53* resembles the shorter hOGA isoform lacking the HAT-like domain, whereas *TaOGA54* is similar to the full-length hOGA (Fig. 1b, supplemental Fig. S2a). The glycoside hydrolase domains of *TaOGA53* and *TaOGA54* share 60% sequence identity with each other and are over 50% identical in amino acid composition to the glycoside hydrolase domain of hOGA and *D. melanogaster* OGA (*DmOGA*). The Asp-Asp motif shown to be important for hOGA activity (65) is conserved in the *TaOGAs* (Fig. 1b, supplemental Fig. S2a). The *TaOGAs* are also both about 40% identical to the structurally characterized bacterial OGA from *Oceanicola granulosus* (*OgOGA*) (66), with which they share a conserved active site (Fig. 1b, supplemental Fig. S2, b and c). Neither *TaOGA53* nor *TaOGA54* appears to have a caspase 3-cleavage site, a feature present in hOGA (Fig. 1a, supplemental Fig. S2a) (37).

For immunodetection of *TaOGT* and the *TaOGAs*, antibodies were raised against two unique peptides within each protein. However, antigen-purified antibodies could only detect their respective recombinant proteins and not endogenous *TaOGT* or *TaOGA53* and *TaOGA54* in lysates by Western blotting or immunoprecipitation. This was probably either due to low expression levels of these proteins or weak affinity of the antibodies toward them. Nevertheless, analysis of published high-resolution proteomics reveals the presence of *TaOGT* and *TaOGA54* in the *Trichoplax* proteome when the organism is cultured under standard culture conditions (67).

Reports have suggested the existence of a ring of putative stem cells at the periphery of the body of *Trichoplax* (53), where specific orthologues of the developmental genes *Hox*, *T-box*, and *Pax* have been shown to be expressed (53, 67–70). Given

that *Ogt* is part of the polycomb group of developmental genes in *Drosophila* (30) and has been shown to be essential for stem cell viability in mice (40), we wanted to investigate localization of OGT in *Trichoplax* to explore its potential function in this basal metazoan. In the absence of a robust antibody for immunofluorescence staining, we performed *in situ* hybridization to localize OGT transcripts in *Trichoplax* whole mounts. Dioxigenin-labeled antisense probes were used and sense controls were performed in parallel. To detect hybridized probes, we used alkaline phosphatase-conjugated anti-dioxigenin antibodies and a substrate that turns purple upon reacting with alkaline phosphatase. In contrast to the transcripts of the aforementioned developmental genes, OGT transcripts were not restricted to the periphery of the organism. Instead, we observed that OGT transcripts were distributed evenly in the organism in samples probed with antisense RNA ($n = 12$) with negligible staining in those probed with the sense control ($n = 12$) (Fig. 1c). This pattern is similar to the expression of the ubiquitous actin (53) and suggests that OGT, which is expressed in several tissues in higher organisms (71), may also be expressed and have functions in the different cell types of a basal organism like *Trichoplax*.

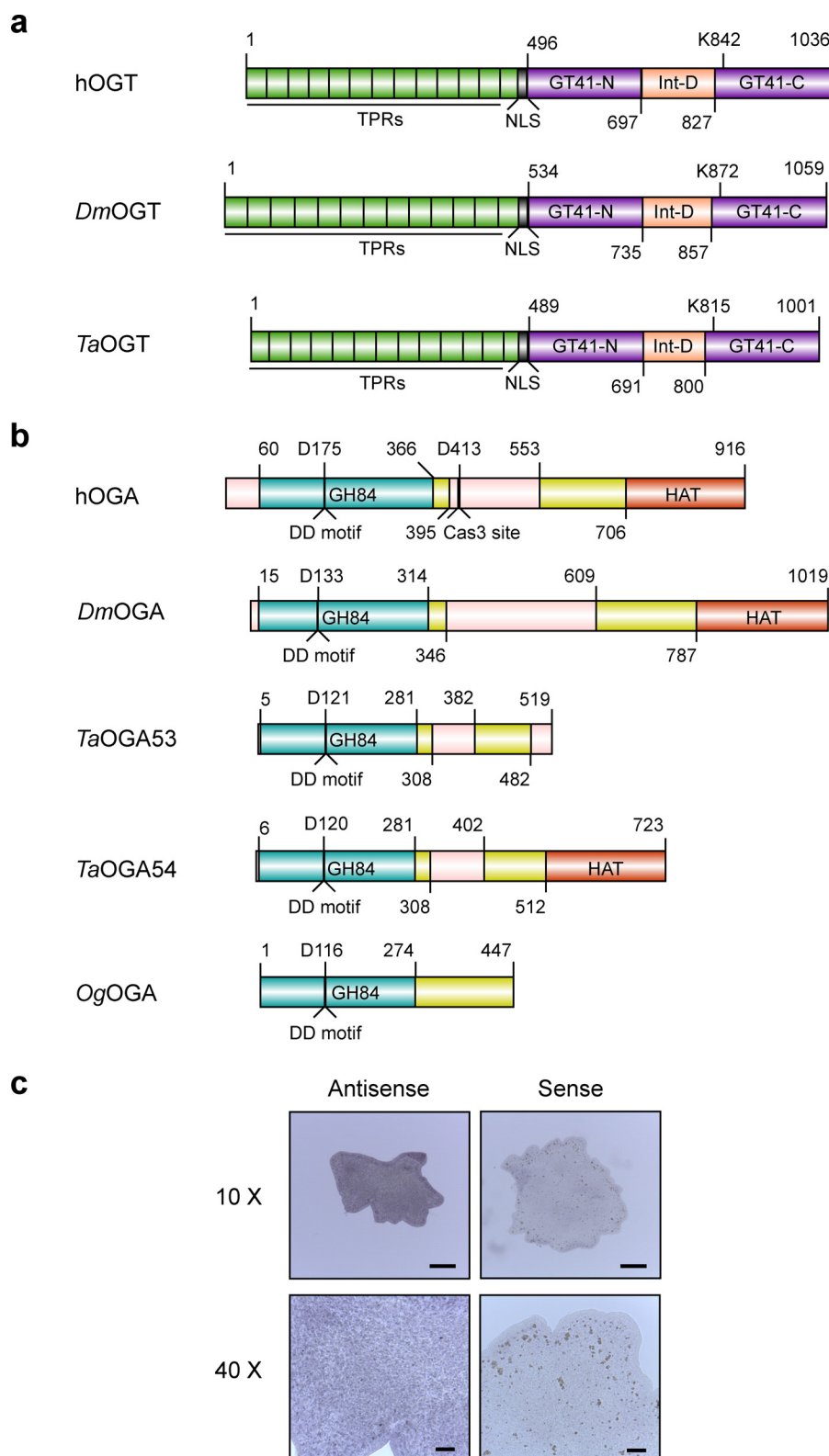
TaOGT Is a Functional O-GlcNAc Transferase—We cloned, recombinantly expressed, and purified the putative *TaOGT* to investigate its activity and elucidate its biochemical properties. The negative control for this experiment was the Lys-815 (*TaOGT*^{K815M}) mutated to Met because the equivalent Lys-842 residue in hOGT is indispensable for catalysis (52). Steady-state kinetics were performed employing a recently published fluorescence assay (48). The K_m for UDP-GlcNAc was measured in the presence of excess peptide substrate (KKENSPAVT-PVSTA, previously used as a substrate to measure the activity of hOGT (48)) and was found to be $13 \pm 2 \mu\text{M}$, within the range reported for hOGT (24, 72–74) (Fig. 2a). *TaOGT* activity is inhibited by the OGT bisubstrate inhibitor Goblin 1 (48) with an IC_{50} (27 μM) comparable with that reported for hOGT (Fig. 2b). Furthermore, *TaOGT*^{WT}, but not the inactive mutant *TaOGT*^{K815M}, could O-GlcNAc modify human CK2 α (hCK2 α), a well characterized hOGT substrate (75–77) *in vitro*, thus validating it as a true OGT orthologue (Fig. 2c). This experiment also revealed that *TaOGT*^{WT}, like its full-length human counterpart (75), undergoes autoglycosylation as evidenced by the reactivity of the anti-O-GlcNAc antibody RL-2 toward *TaOGT*^{WT} but not *TaOGT*^{K815M} (Fig. 2c).

TaOGT Rescues Drosophila supersex combs (sxc) Lethality—*Drosophila* OGT mutants, also known as *supersex combs (sxc)* mutants, die as pharate adults and this lethality can be rescued by ubiquitous expression of transgenic wild type *DmOGT* in *sxc* transheterozygotes (31). We used this approach to investigate the functional equivalence of *TaOGT* and *DmOGT*. Initial experiments were performed in S2 cells where endogenous OGT was knocked down using RNAi directed towards the 3' UTR of *DmOGT* and cells were transfected with plasmids carrying either *TaOGT*^{WT} or the catalytically inactive *TaOGT*^{K815M}. O-GlcNAc levels in cells transfected with *TaOGT*^{WT}, but not *TaOGT*^{K815M}, were restored to levels comparable with cells transfected with *DmOGT* (Fig. 3a). Strikingly, in the context of the whole organism, the number of *sxc*

O-GlcNAc in the Simplest Known Animal

transheterozygotes recovered on rescue with *TaOGT* (13% of total progeny) was comparable with that of the *DmOGT* (26% of total progeny). The level of rescue with *DmOGT* is twice as that of *TaOGT*^{WT} because the transgenic line used in the case of *DmOGT* was homozygous (Fig. 3*b*, Table 1). In the control crosses lacking either the driver or the transgene, no adult *sxc*¹/

*sxc*⁶ transheterozygotes were recovered. *sxc* is a maternal effect gene and the rescue by *TaOGT* to produce F1 progeny is the rescue of the zygotic requirement of OGT. To assess whether the maternal OGT function could also be rescued by *TaOGT*, the rescued F1 males were crossed with rescued F1 females. The only completely functional OGT in this cross is the *TaOGT*^{WT}



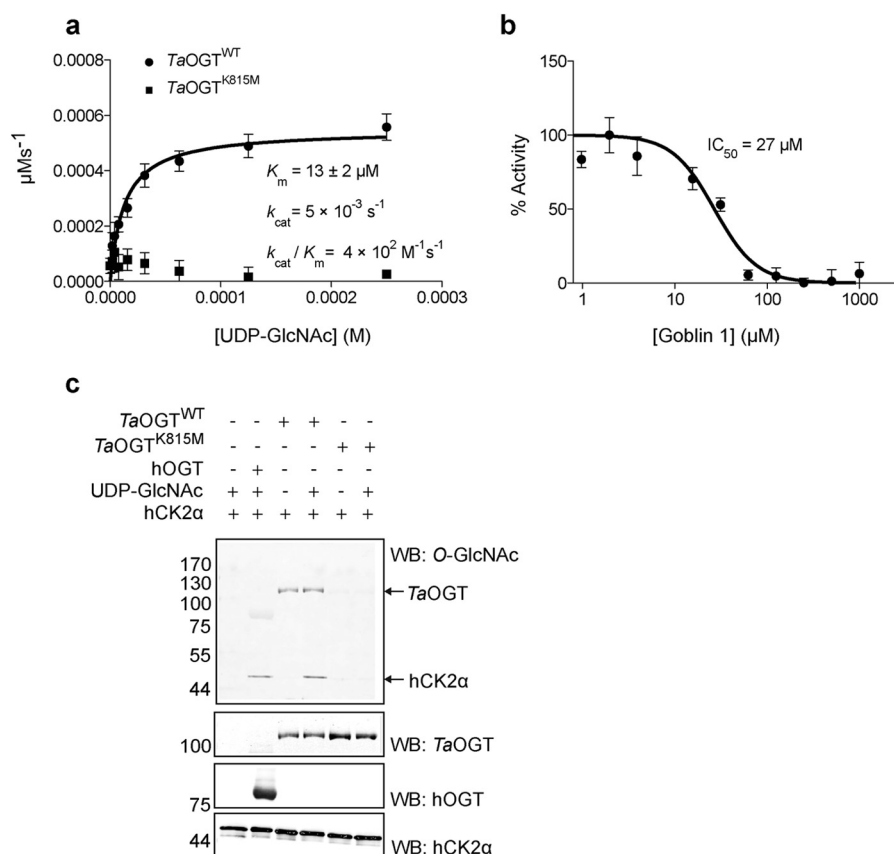


FIGURE 2. $TaOGT$ is a functional O-GlcNAc transferase. *a*, Michaelis-Menten kinetics of $TaOGT$ measured using the peptide substrate KKENSAPVTPVSTA and varying amounts of UDP-GlcNAc. Reactions were carried out for 75 min at room temperature and read after the addition of a compound that fluoresces upon binding to the reaction product UDP (48–50). Data points were fitted to the Michaelis-Menten equation using Prism (GraphPad). Experiments were performed in triplicate and error bars represent mean \pm S.E. *b*, IC_{50} of the bisubstrate inhibitor Goblin 1 for $TaOGT$. IC_{50} was measured using UDP-GlcNAc at a concentration equal to the K_m and varying amounts of the inhibitor. Highest activity in the absence of inhibitors is arbitrarily set as 100%. Data points were fitted to a three-parameter equation for dose-dependent inhibition using Prism (GraphPad). Experiments were performed in triplicate and error bars represent mean \pm S.E. *c*, *in vitro* O-GlcNAcylation of hCK2α by $TaOGT$ and autoglycosylation of $TaOGT$ detected by Western blotting using the anti-O-GlcNAc antibody RL-2. hCK2α was incubated with $TaOGT$ and a molar excess of UDP-GlcNAc at room temperature for 1.5 h. Negative controls include hCK2α treated with the catalytically inactive $TaOGT^{K815M}$ or with $TaOGT^{WT}$ in the absence of the donor substrate UDP-GlcNAc. hCK2α treated with hOGT(312–1031) was used as a positive control. WB, Western blot.

driven by tubulin::GAL4. Fertile F2 progeny were recovered from this cross establishing that $TaOGT$ could also substitute for the maternal requirement of *sxc* in early *Drosophila* development. The catalytically inactive $TaOGT^{K815M}$, on the other hand, does not rescue the *sxc* lethality phenotype. The level of rescue of the catalytic activity of $TaOGT$ was investigated by performing Western blots against total O-GlcNAc using adult fly lysates. The level of total O-GlcNAc both in F1 and F2 $TaOGT^{WT}$ rescued *sxc* adults is comparable with that of *DmOGT* rescued *sxc* mutants (Fig. 3c), implying that $TaOGT$ is a fully functional OGT orthologue.

$TaOGA53$ and $TaOGA54$ Are Functional O-GlcNAc Transferases—To test whether the putative $TaOGA53$ and $TaOGA54$ are active enzymes, we recombinantly expressed and purified

them from *E. coli*. The negative controls were the Ala mutants of the predicted catalytic residues in the Asp-Asp motif (65) of the enzymes (Asp¹²⁰, $TaOGA53^{D120A}$ and Asp¹²¹, $TaOGA54^{D121A}$). Steady-state kinetics experiments were performed using the fluorogenic pseudo-substrate 4MU-NAG. A Michaelis constant K_m of $78 \pm 5 \mu\text{M}$ and a turnover number k_{cat} of $3 \times 10^{-3} \text{ s}^{-1}$, were obtained for $TaOGA53$, the shorter of the $TaOGAs$ (Fig. 4a), whereas $TaOGA54$, the longer enzyme containing the HAT-like domain, was found to have a K_m of $2.0 \pm 0.1 \text{ mM}$ and a turnover number k_{cat} of 1 s^{-1} (Fig. 4b). In contrast, the long hOGA isoform has been reported to have a lower K_m than the shorter isoform (78, 79). The catalytic efficiency (k_{cat}/K_m) of $TaOGA54$ ($5 \times 10^2 \text{ M}^{-1} \text{ s}^{-1}$) is 12.5-fold higher than that of $TaOGA53$ ($40 \text{ M}^{-1} \text{ s}^{-1}$). The reduced catalytic activity indicated

FIGURE 1. *Trichoplax* possesses OGT and OGA orthologues. *a*, schematic showing the domains of $TaOGT$ compared with hOGT and *DmOGT*. The TPR region of the proteins is shown in green, the N- and C-terminal catalytic lobes (GT41-N and GT41-C) in purple, and the intervening domain (Int-D) in peach. The conserved lysine residue required for catalytic activity of the OGTs is shown, as is the conserved nuclear localization signal (NLS) in the proteins. *b*, schematic showing the domain architecture of the $TaOGAs$ compared with hOGA, *DmOGA*, and *OgOGA* (a structurally characterized bacterial OGA with high sequence conservation with hOGA (66)). The catalytic domain with glycoside hydrolase activity (GH84) is shown in blue, the middle domain in yellow, and the HAT-like domain (HAT) in orange. The Asp-Asp motif (DD motif) required for activity and the catalytic residue within it are depicted. The caspase 3 cleavage site of hOGA is also shown. Regions of predicted structural disorder within the proteins are shown in pale salmon. *c*, localization of $TaOGT$ transcripts analyzed by whole mount *in situ* hybridization using dioxigenin-labeled probes. Hybridized probes detected using alkaline phosphatase (AP)-conjugated anti-dioxigenin antibody and the AP substrate BM purple. Purple staining throughout the organism shows ubiquitous presence of $TaOGT$ transcripts. Scale bars: top panels, 100 μm ; bottom panels, 20 μm .

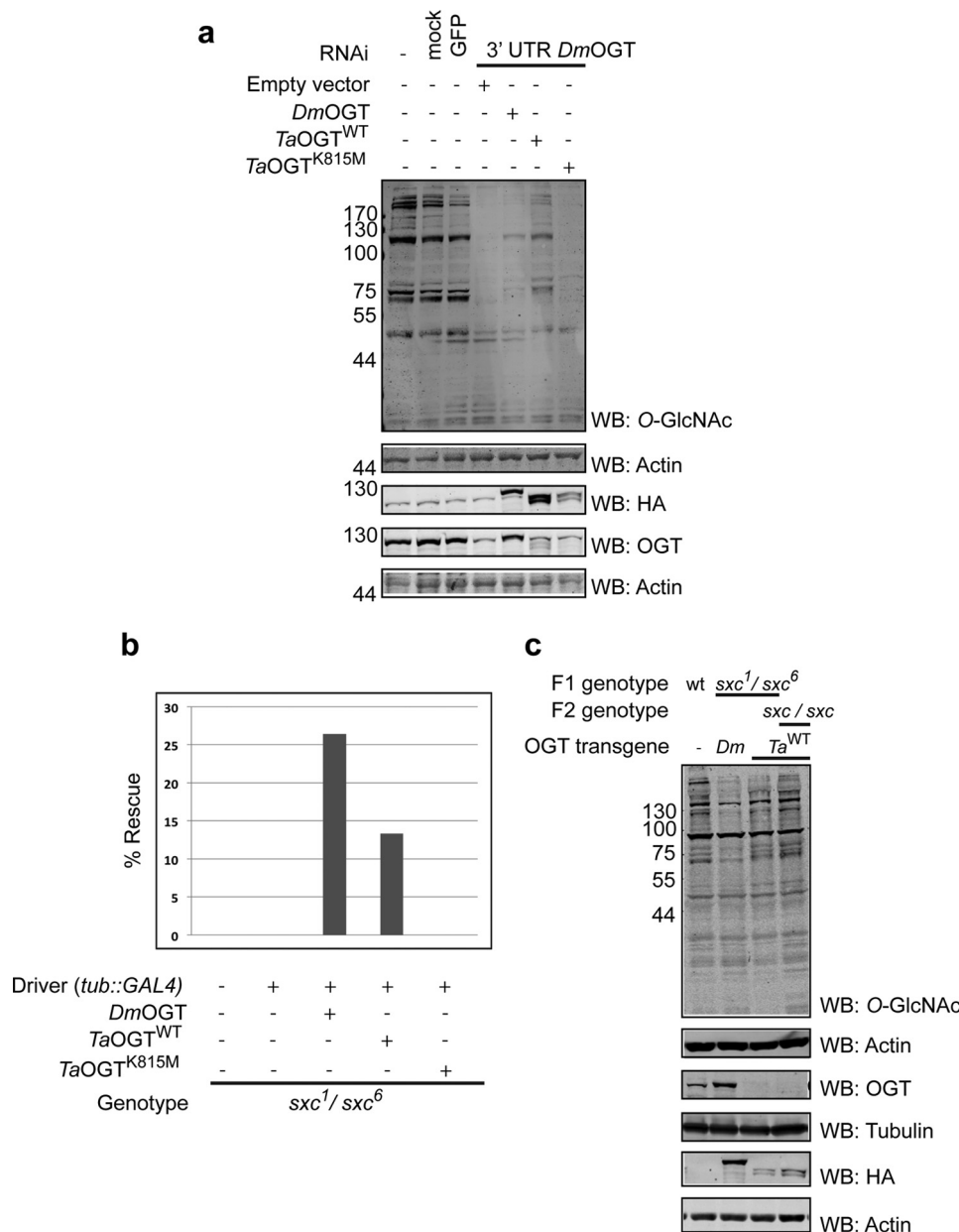


FIGURE 3. *Ta*OGT can rescue the lethality of *Drosophila supersex combs* (*sxc*) mutants. *a*, *Ta*OGT^{WT} restores O-GlcNAc levels in S2 cells lacking endogenous OGT. RNAi was used to knockdown endogenous OGT in S2 cells. GFP RNAi was used as a control. Cells were then transfected with plasmids carrying HA-tagged *Dm*OGT, *Ta*OGT^{WT}, or catalytically inactive *Ta*OGT^{K815M}. Cells were lysed and total lysates were probed by Western blotting using the specified antibodies. *b*, quantification of rescue to adulthood on driving *Dm*OGT, *Ta*OGT^{WT}, or *Ta*OGT^{K815M} transgenes in *sxc*¹/*sxc*⁶ mutants. The number of *sxc* transheterozygotes recovered on rescue with *Ta*OGT^{WT} is comparable with that of the *Dm*OGT. The level of rescue with *Dm*OGT is twice as that of *Ta*OGT^{WT} because the transgenic line used in the case of *Dm*OGT was homozygous. *c*, O-GlcNAc levels in flies expressing *Ta*OGT^{WT} are comparable with those expressing *Dm*OGT. Total lysates from *w*¹¹¹⁸ (wt), rescued F1 *sxc*¹/*sxc*⁶ transheterozygotes, or F2 *sxc*/*sxc* flies expressing HA-tagged UAS::*Dm*OGT or UAS::*Ta*OGT^{WT} under the control of tubulin::GAL4 were probed by Western blotting using the specified antibodies. WB, Western blot.

TABLE 1
Rescue of *sxc* lethality by *Ta*OGT

Crosses were setup up with flies of the indicated genotypes and transferred into fresh vials every 3–4 days. Adults emerging from the crosses were scored for the presence of second and third chromosome balancers/marker, CyO and MKRS or TM6. Flies that did not possess any of the balancers/markers (+; +) were the rescued *sxc*¹/*sxc*⁶ transheterozygotes. Control crosses with flies lacking either the driver (tubulin::GAL4) or any of the OGT transgenes do not yield any non-CyO adults.

Parental cross	Total adults	CyO; TM6	CyO; MKRS	CyO; MKRS/TM6	CyO; +	+; +
<i>sxc</i> ⁶ /CyO; <i>tub::GAL4</i> /TM6 ♀ × <i>sxc</i> ¹ /CyO; MKRS/TM6 ♂	119	26	54	39	NA ^a	0
<i>sxc</i> ⁶ /CyO; MKRS/TM6 ♀ × <i>sxc</i> ¹ /CyO; UAS:: <i>Ta</i> OGT ^{WT} /TM6 ♂	195	54	97	44	NA	0
<i>sxc</i> ⁶ /CyO; <i>tub::GAL4</i> /TM6 ♀ × <i>sxc</i> ¹ /CyO; UAS:: <i>Dm</i> OGT ^{WT} ♂	174	76	NA	NA	52	46
<i>sxc</i> ⁶ /CyO; <i>tub::GAL4</i> /TM6 ♀ × <i>sxc</i> ¹ /CyO; UAS:: <i>Ta</i> OGT ^{WT} /TM6 ♂	203	120	NA	NA	50	27
<i>sxc</i> ⁶ /CyO; <i>tub::GAL4</i> /TM6 ♀ × <i>sxc</i> ¹ /CyO; UAS:: <i>Ta</i> OGT ^{K815M} /TM6 ♂	131	94	NA	NA	37	0

^a NA, not applicable.

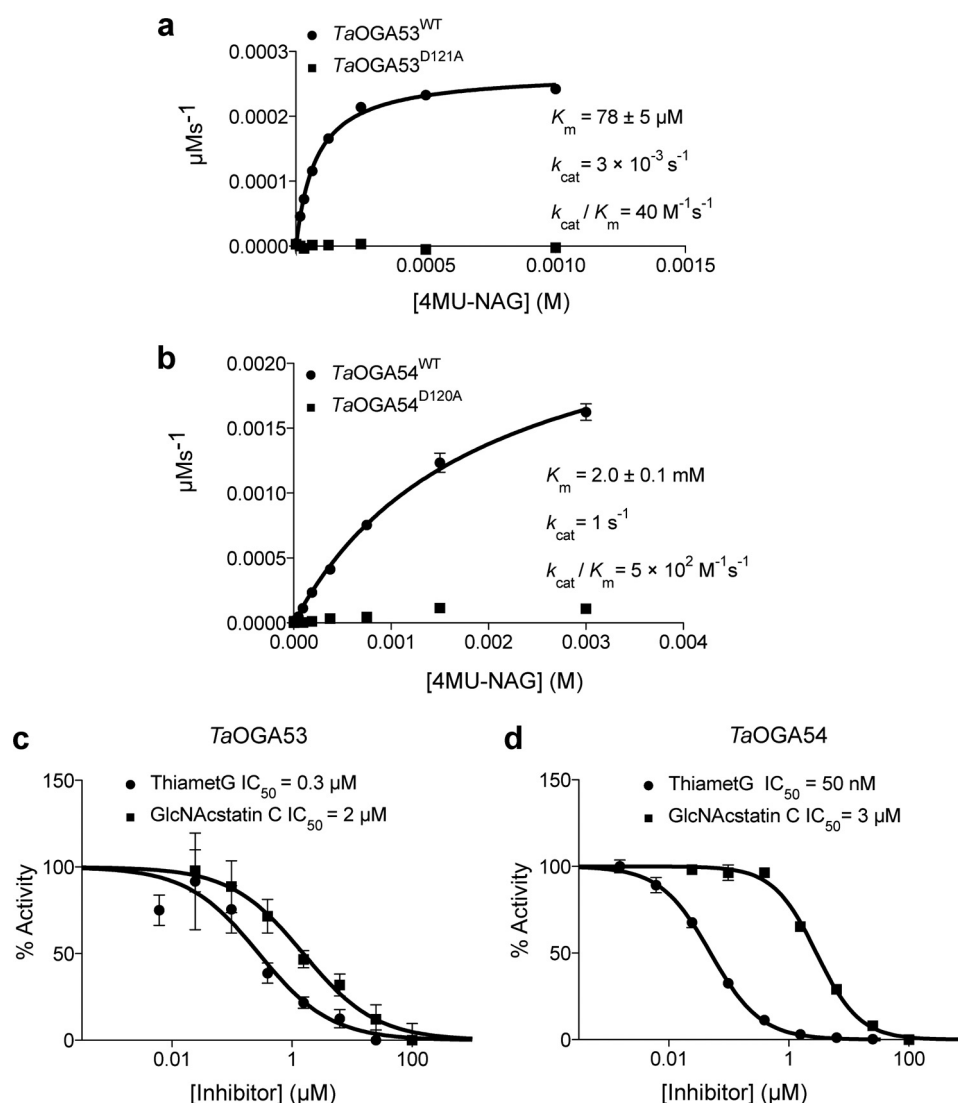


FIGURE 4. *TaOGA53* and *TaOGA54* are functional O-GlcNAcases. *a*, Michaelis-Menten kinetics of *TaOGA53* using varying amounts of 4MU-NAG. Reactions were carried out for 120 min at room temperature. Data points were fitted to the Michaelis-Menten equation using Prism (GraphPad). Experiments were performed in triplicate and error bars represent mean \pm S.E. *b*, Michaelis-Menten kinetics of *TaOGA54* measured using varying amounts of the fluorescent substrate 4MU-NAG. Reactions were carried out for 30 min at room temperature. Data points were fitted to the Michaelis-Menten equation using Prism (GraphPad). Experiments were performed in triplicate and error bars represent mean \pm S.E. *c*, IC_{50} of Thiamet G and GlcNAcstatin C for *TaOGA53*. IC_{50} values were measured using 4MU-NAG at a concentration equal to the K_m and varying amounts of inhibitors. Highest activity in the absence of inhibitors is arbitrarily set as 100%. Data points were fitted to a three-parameter equation for dose-dependent inhibition using Prism (GraphPad). Experiments were performed in triplicate and error bars represent mean \pm S.E. *d*, IC_{50} of Thiamet G and GlcNAcstatin C for *TaOGA54*. IC_{50} values were measured using 4MU-NAG at a concentration equal to the K_m and varying amounts of inhibitors. Highest activity in the absence of inhibitors is arbitrarily set as 100%. Data points were fitted to a three-parameter equation for dose-dependent inhibition using Prism (GraphPad). Experiments were performed in triplicate and error bars represent mean \pm S.E.

by the ~ 300 -fold decrease in k_{cat} of *TaOGA53* compared with *TaOGA54* is comparable with the reduced catalytic activity of the short *versus* full-length isoforms of hOGA reported previously (78, 79). The activities of both *TaOGA53* and *TaOGA54* are inhibited by the well characterized OGA inhibitors GlcNAcstatin C (80, 81) and Thiamet G (82) (Fig. 4, *c* and *d*).

To further confirm that *TaOGA53* and *TaOGA54* are active, *in vitro* O-GlcNAcylated hCK2 α and HEK293/*Drosophila* S2 cell lysates were treated with increasing amounts of the enzymes and probed for O-GlcNAc using the RL-2 antibody. Samples were also treated with the catalytically inactive *TaOGA53*^{D120A} and *TaOGA54*^{D121A}. Treatment of samples with *TaOGA53*^{WT} did not lead to a noticeable decrease in O-GlcNAc signal (Fig. 5, *a* and *c*). Under the same experimental

conditions, treatment with *TaOGA54*^{WT}, but not its inactive counterpart *TaOGA54*^{D121A}, resulted in a dose-dependent decrease in O-GlcNAc signal obtained in comparison to untreated controls (Fig. 5, *b* and *d*). To determine specificity of RL-2 to O-GlcNAc, lysates were also independently probed with RL-2 antibody preincubated with 0.5 M GlcNAc or secondary antibody alone. The difference in activity observed for *TaOGA53* and *TaOGA54* on lysates is not unexpected given the kinetic parameters of these enzymes. The ability of *TaOGA54* to de-O-GlcNAcylate HEK293 and S2 cell lysates demonstrates that *Trichoplax* possesses a functional orthologue of metazoan OGA.

***Trichoplax* Possesses O-GlcNAcylated Proteins**—Having established that *Trichoplax* expresses functional orthologues

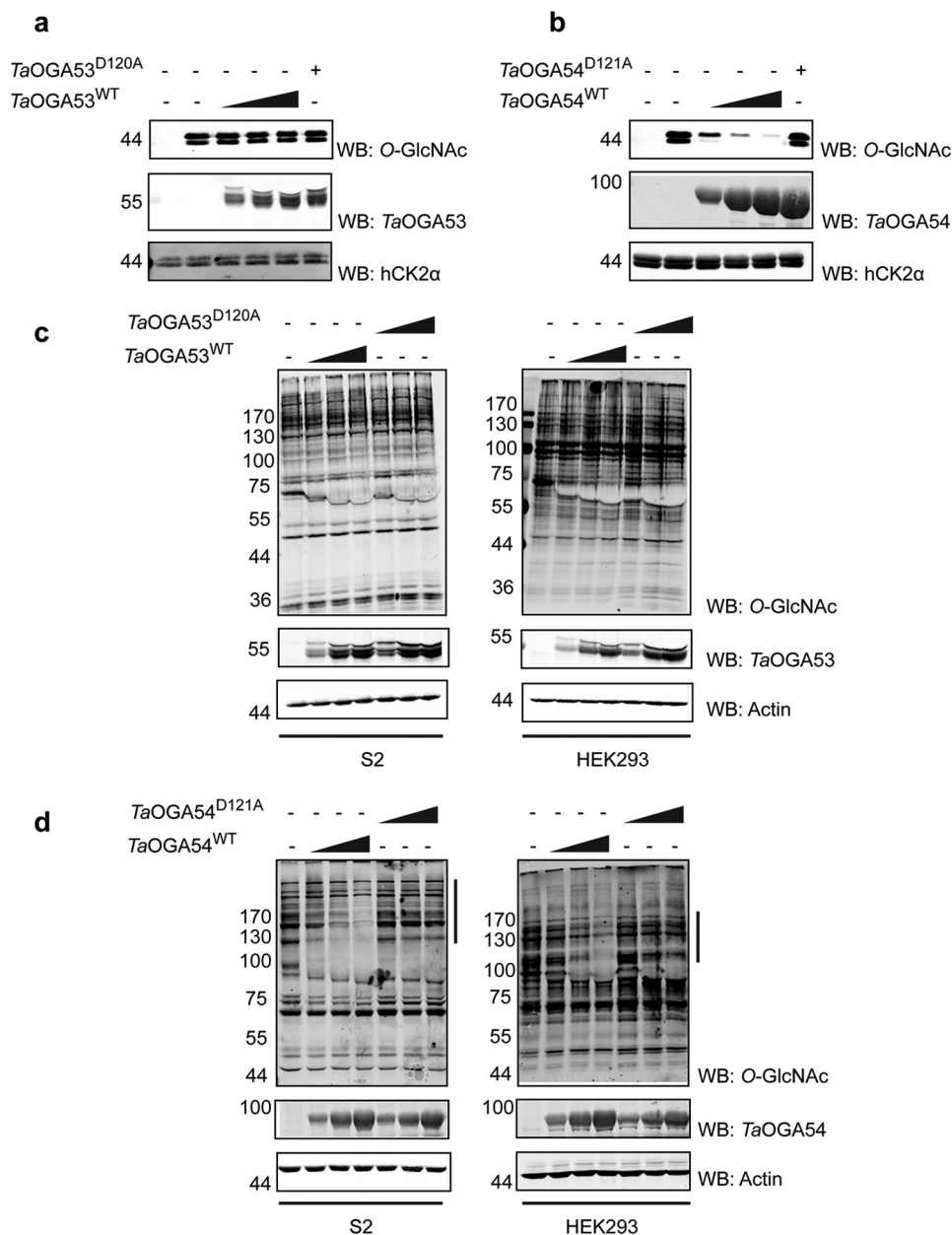


FIGURE 5. **In vitro** activity of *TaOGA53* and *TaOGA54*. *a*, activity of *TaOGA53* (5, 10, and 15 μ g) on *in vitro* O-GlcNAcylated hCK2 α detected by Western blotting using the anti-O-GlcNAc antibody RL-2. Reactions were carried out at room temperature for 4 h. A sample treated with 15 μ g of the inactive mutant *TaOGA53*^{D120A} was included as a negative control. Non-O-GlcNAcylated hCK2 α (first lane) was also included as a negative control. *b*, activity of *TaOGA54* (5, 10, and 15 μ g) on *in vitro* O-GlcNAcylated hCK2 α detected by Western blotting using the anti-O-GlcNAc antibody RL-2. Reactions were carried out at room temperature for 4 h. A sample treated with 15 μ g of the inactive mutant *TaOGA53*^{D120A} was included as a negative control. Non-O-GlcNAcylated hCK2 α (first lane) was also included as a negative control. *c*, activity of *TaOGA53* (5, 10, and 15 μ g) on 20 μ g of S2 and HEK293 cell lysates detected by Western blotting using the anti-O-GlcNAc antibody RL-2. Reactions were carried out at room temperature for 4 h. Lysates treated with the inactive mutant *TaOGA53*^{D120A} were included as a negative control. *d*, activity of *TaOGA54* (5, 10, and 15 μ g) on 20 μ g of S2 and HEK293 cell lysates detected by Western blotting using the anti-O-GlcNAc antibody RL-2. Reactions were carried out at room temperature for 4 h. Lysates treated with the inactive mutant *TaOGA54*^{D121A} were included as a negative control. Reduction in specific O-GlcNAc signal as a consequence of treatment with *TaOGA54*^{WT} is indicated by lines to the right of the RL-2 blots.

of OGT and OGA, we investigated the presence of O-GlcNAcylated proteins in the organism by Western blotting using the anti-O-GlcNAc antibody CTD110.6. *Trichoplax* lysates were probed for O-GlcNAc alongside lysates of *R. salina*, the algal food source used to culture *Trichoplax*, as a negative control. *Trichoplax* lysates showed reactivity toward the antibody, whereas *Rhodomonas* lysates did not, confirming that CTD110.6 reactive proteins were exclusively of *Trichoplax* origin (Fig. 6*a*). Specificity of the signal toward O-GlcNAc was

determined by preincubating CTD110.6 with 0.5 M GlcNAc, which competed away CTD110.6 reactivity (Fig. 6*b*). The presence of O-GlcNAcylated proteins in *Trichoplax* was further confirmed using the alternative "Click-It" approach, whereby O-GlcNAc residues are labeled using a mutant galactosyltransferase (Gal-T1^{Y289L}) (83) with azido-modified galactose, which is then reacted with biotin-alkyne via copper-dependent cycloaddition and detected by Western blotting using peroxidase-conjugated streptavidin (84).

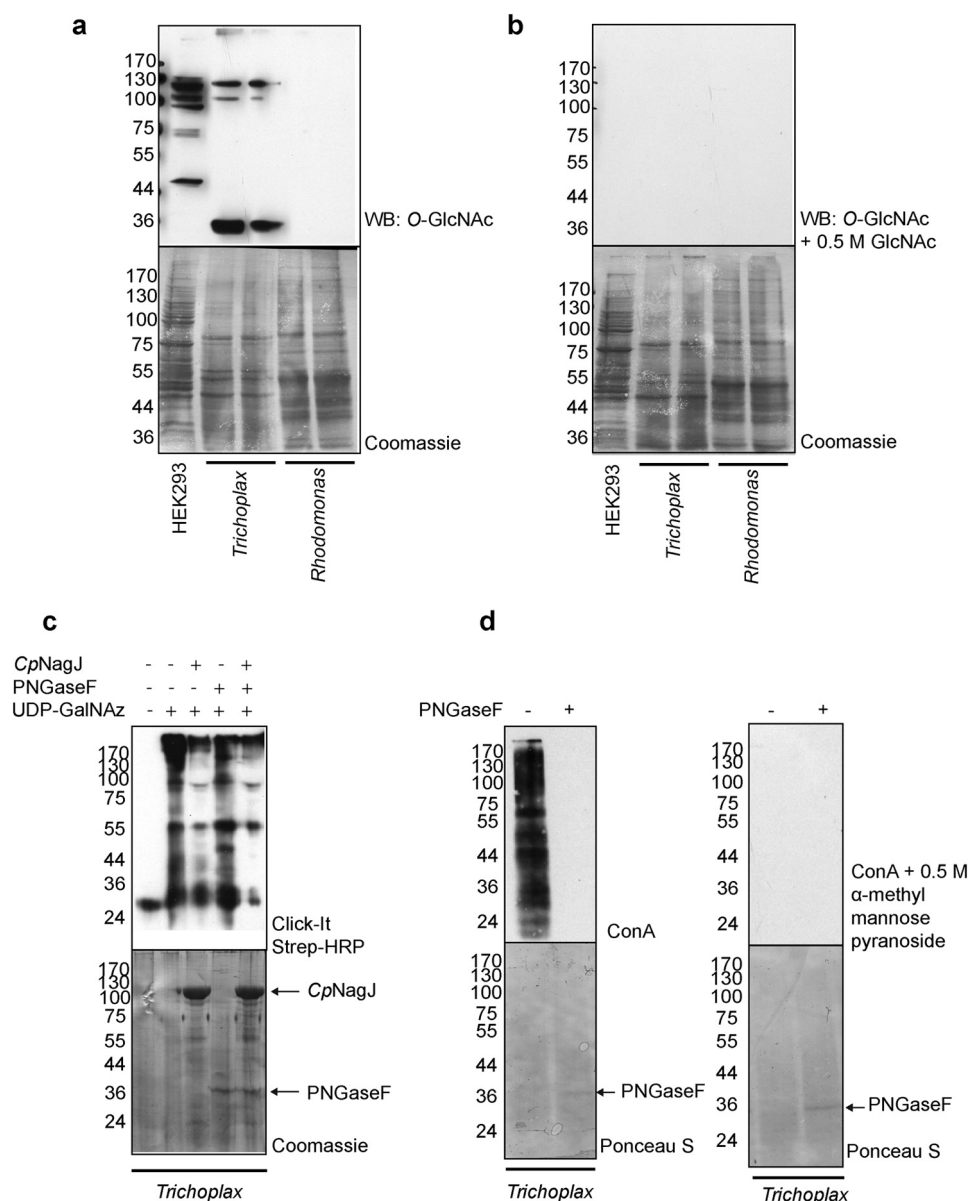


FIGURE 6. *Trichoplax* possesses O-GlcNAc-modified proteins. *a*, *Trichoplax* total lysates were subjected to Western blotting using the anti O-GlcNAc antibody CTD110.6. HEK293 cell lysates were used as a positive control and *Rhodomonas* lysates were used to ensure the O-GlcNAc signal from *Trichoplax* lysates were specific to *Trichoplax* proteins and not contaminating algal proteins in the lysate. *b*, lysates probed with anti-O-GlcNAc antibody preincubated with 0.5 M GlcNAc to show specificity of CTD110.6 antibody to GlcNAc. *c*, *Trichoplax* lysates treated with GalT1^{Y289L} to label O-GlcNAc residues with azido-modified galactose (GalNAz), which in turn is attached to biotin via click chemistry and probed with peroxidase-conjugated streptavidin (strep-HRP) to detect O-GlcNAcylated proteins. Lysates were treated with the bacterial O-GlcNAcase CpNagJ and/or PNGase F prior to labeling with GalNAz for specific detection of O-GlcNAcylated proteins. *d*, *Trichoplax* lysates subjected to PNGase F treatment were probed with concanavalin A (ConA) to confirm activity of PNGase F on the N-glycans of *Trichoplax*. The specificity of ConA was assessed by competing it with 0.5 M α -methyl mannose pyranoside.

However, the Click-It method could potentially identify any glycosylated protein containing a terminal GlcNAc. *Trichoplax* lysates were therefore treated with PNGase F or CpNagJ, a bacterial OGA (51), to specifically remove N-linked glycans or O-GlcNAc, respectively, prior to performing the Click-It reactions, to ensure specific detection of O-GlcNAc. Although PNGase F treatment did not result in significant reduction in signal obtained with streptavidin-HRP, CpNagJ treatment led to a reduction in signal, establishing the specificity of the results obtained with the Click-It method (Fig. 6c). PNGase F-treated lysates were also

probed with the lectin concanavalin A (ConA) to ensure N-linked glycans were successfully stripped (Fig. 6d).

DISCUSSION

Our data show that the basal metazoan *Trichoplax* expresses functional OGT and OGA and also possesses O-GlcNAcylated proteins. Our results suggest that OGT may have a ubiquitous role in *Trichoplax* because its transcripts do not exclusively localize at specific regions of the organism. It is remarkable, given the minimalistic morphology of *Trichoplax*, that TaOGT is able to rescue the lethality of *Drosophila* OGT null mutants.

This suggests roles for OGT and protein O-GlcNAcylation in evolutionarily conserved processes in *Trichoplax*.

Trichoplax is unusual among metazoa in that it encodes two orthologues of OGA. It is possible given the biochemical properties of the shorter TaOGA53 that this is an inactive enzyme with regulatory or scaffolding functions. Although the K_m for TaOGA54 toward the pseudosubstrate 4MU-NAG is about 25-fold higher compared with hOGA (85), its activity on human cell lysates is comparable with that reported for hOGA previously (78), indicating functional conservation of OGA activity throughout metazoan evolution.

The phylogenetic position of *Trichoplax* at the base of metazoa has allowed it to be used in studies investigating the evolution of human cellular pathways and proteins (86, 87). A recent study used comparative genomics to identify metazoan-specific genes defined on the basis of being present in all metazoans including *Trichoplax*, but being absent in other eukaryotes (88). Its presence in *Trichoplax* but not in protists, adds *oga* to this repertoire of metazoan-specific genes. Although the presence of active OGT and O-GlcNAcylated proteins in plants and protists (55, 89) implies a eukaryote-specific role for intracellular O-GlcNAcylation, it is possible that the post-translational modification is dynamic and reversible only in metazoa. Alternatively, an as yet undiscovered enzyme with low sequence homology to OGA may be responsible for O-GlcNAc hydrolysis in protists and plants.

Signal transduction, in part through some types of post-translational modifications of proteins is thought to be one of the prerequisites for multicellularity in metazoa (88, 89). A recent study found higher levels of tyrosine phosphorylation in the proteome of *Trichoplax* than present in more basal or complex organisms, and ascribed it to the appearance of dedicated tyrosine kinases at the onset of metazoan multicellularity (67). Similarly, the acquisition of OGA by *Trichoplax* (and other metazoa) may have enabled the fine-tuning of signal transduction partly via facilitating interplay between O-GlcNAcylation and phosphorylation that is known to exist in other organisms (3–5).

We show that *T. adhaerens*, the simplest known animal, is a suitable reductionist model, as it is the most basal organism to possess the machinery required for reversible protein O-GlcNAcylation. Despite lacking the genetic tractability of other model systems, *Trichoplax* presents as a useful system to identify conserved O-GlcNAc proteins and help shape our understanding of the evolutionary roles for reversible O-GlcNAcylation.

Acknowledgments—We thank Leo Buss for providing *T. adhaerens* and R. salina and for advice on maintaining them in culture. We thank Bernd Schierwater for advice with performing *in situ* hybridization experiments.

REFERENCES

- Hart, G. W., Slawson, C., Ramirez-Correa, G., and Lagerlof, O. (2011) Cross talk between O-GlcNAcylation and phosphorylation: roles in signaling, transcription, and chronic disease. *Annu. Rev. Biochem.* **80**, 825–858
- Torres, C. R., and Hart, G. W. (1984) Topography and polypeptide distribution of terminal N-acetylglucosamine residues on the surfaces of intact lymphocytes: evidence for O-linked GlcNAc. *J. Biol. Chem.* **259**, 3308–3317
- Trinidad, J. C., Barkan, D. T., Gullledge, B. F., Thalhammer, A., Sali, A., Schoepfer, R., and Burlingame, A. L. (2012) Global identification and characterization of both O-GlcNAcylation and phosphorylation at the murine synapse. *Mol. Cell. Proteomics* **11**, 215–229
- Wang, Z., Gueck, M., and Hart, G. W. (2008) Cross-talk between GlcNAcylation and phosphorylation: site-specific phosphorylation dynamics in response to globally elevated O-GlcNAc. *Proc. Natl. Acad. Sci. U.S.A.* **105**, 13793–13798
- Hu, P., Shimoji, S., and Hart, G. W. (2010) Site-specific interplay between O-GlcNAcylation and phosphorylation in cellular regulation. *FEBS Lett.* **584**, 2526–2538
- Wells, L., Kreppel, L. K., Comer, F. I., Wadzinski, B. E., and Hart, G. W. (2004) O-GlcNAc transferase is in a functional complex with protein phosphatase 1 catalytic subunits. *J. Biol. Chem.* **279**, 38466–38470
- Dias, W. B., Cheung, W. D., Wang, Z., and Hart, G. W. (2009) Regulation of calcium/calmodulin-dependent kinase IV by O-GlcNAc modification. *J. Biol. Chem.* **284**, 21327–21337
- Bullen, J. W., Balsbaugh, J. L., Chanda, D., Shabanowitz, J., Hunt, D. F., Neumann, D., and Hart, G. W. (2014) Cross-talk between two essential nutrient-sensitive enzymes: O-GlcNAc transferase (OGT) and AMP-activated protein kinase (AMPK). *J. Biol. Chem.* **289**, 10592–10606
- Erickson, J. R., Pereira, L., Wang, L., Han, G., Ferguson, A., Dao, K., Copeland, R. J., Despa, F., Hart, G. W., Ripplinger, C. M., and Bers, D. M. (2013) Diabetic hyperglycaemia activates CaMKII and arrhythmias by O-linked glycosylation. *Nature* **502**, 372–376
- Sümege, M., Hunyadi-Gulyás, E., Medzihradsky, K. F., and Udvardy, A. (2003) 26 S proteasome subunits are O-linked N-acetylglucosamine-modified in *Drosophila melanogaster*. *Biochem. Biophys. Res. Commun.* **312**, 1284–1289
- Zachara, N. E., and Hart, G. W. (2004) O-GlcNAc a sensor of cellular state: the role of nucleocytoplasmic glycosylation in modulating cellular function in response to nutrition and stress. *Biochim. Biophys. Acta* **1673**, 13–28
- Zachara, N. E., O'Donnell, N., Cheung, W. D., Mercer, J. J., Marth, J. D., and Hart, G. W. (2004) Dynamic O-GlcNAc modification of nucleocytoplasmic proteins in response to stress. A survival response of mammalian cells. *J. Biol. Chem.* **279**, 30133–30142
- Liu, J., Pang, Y., Chang, T., Bounelis, P., Chatham, J. C., and Marchase, R. B. (2006) Increased hexosamine biosynthesis and protein O-GlcNAc levels associated with myocardial protection against calcium paradox and ischemia. *J. Mol. Cell. Cardiol.* **40**, 303–312
- Jackson, S. P., and Tjian, R. (1989) Purification and analysis of RNA polymerase-II transcription factors by using wheat-germ agglutinin affinity chromatography. *Proc. Natl. Acad. Sci. U.S.A.* **86**, 1781–1785
- Sakabe, K., and Hart, G. W. (2010) O-GlcNAc transferase regulates mitotic chromatin dynamics. *J. Biol. Chem.* **285**, 34460–34468
- Sakabe, K., Wang, Z., and Hart, G. W. (2010) β -N-Acetylglucosamine (O-GlcNAc) is part of the histone code. *Proc. Natl. Acad. Sci. U.S.A.* **107**, 19915–19920
- Yang, X., Zhang, F., and Kudlow, J. E. (2002) Recruitment of O-GlcNAc transferase to promoters by corepressor mSin3A: coupling protein O-GlcNAcylation to transcriptional repression. *Cell* **110**, 69–80
- Chen, Q., Chen, Y., Bian, C., Fujiki, R., and Yu, X. (2013) TET2 promotes histone O-GlcNAcylation during gene transcription. *Nature* **493**, 561–564
- Deplus, R., Delatte, B., Schwinn, M. K., Defrance, M., Méndez, J., Murphy, N., Dawson, M. A., Volkmar, M., Putmans, P., Calonne, E., Shih, A. H., Levine, R. L., Bernard, O., Mercher, T., Solary, E., Urh, M., Daniels, D. L., and Fuks, F. (2013) TET2 and TET3 regulate GlcNAcylation and H3K4 methylation through OGT and SET1/COMPASS. *EMBO J.* **32**, 645–655
- Slawson, C., Copeland, R. J., and Hart, G. W. (2010) O-GlcNAc signaling: a metabolic link between diabetes and cancer? *Trends Biochem. Sci.* **35**, 547–555
- Haltiwanger, R. S., Holt, G. D., and Hart, G. W. (1990) Enzymatic addition

- of O-GlcNAc to nuclear and cytoplasmic proteins: identification of a uridine diphospho-*N*-acetylglucosamine:peptide β -*N*-acetylglucosaminyltransferase. *J. Biol. Chem.* **265**, 2563–2568
22. Starr, C. M., and Hanover, J. A. (1990) Glycosylation of nuclear pore protein p62: reticulocyte lysate catalyzes O-linked *N*-acetylglucosamine addition *in vitro*. *J. Biol. Chem.* **265**, 6868–6873
 23. Dong, D. L., and Hart, G. W. (1994) Purification and characterization of an O-GlcNAc selective *N*-acetyl- β -D-glucosaminidase from rat spleen cytosol. *J. Biol. Chem.* **269**, 19321–19330
 24. Haltiwanger, R. S., Blomberg, M. A., and Hart, G. W. (1992) Glycosylation of nuclear and cytoplasmic proteins: purification and characterization of a uridine diphospho-*N*-acetylglucosamine:polypeptide β -*N*-acetylglucosaminyltransferase. *J. Biol. Chem.* **267**, 9005–9013
 25. Kreppel, L. K., Blomberg, M. A., and Hart, G. W. (1997) Dynamic glycosylation of nuclear and cytosolic proteins - Cloning and characterization of a unique O-GlcNAc transferase with multiple tetratricopeptide repeats. *J. Biol. Chem.* **272**, 9308–9315
 26. Gao, Y., Wells, L., Comer, F. I., Parker, G. J., and Hart, G. W. (2001) Dynamic O-glycosylation of nuclear and cytosolic proteins: cloning and characterization of a neutral, cytosolic β -*N*-acetylglucosaminidase from human brain. *J. Biol. Chem.* **276**, 9838–9845
 27. Hanover, J. A., Yu, S., Lubas, W. B., Shin, S. H., Ragano-Caracciola, M., Kochran, J., and Love, D. C. (2003) Mitochondrial and nucleocytoplasmic isoforms of O-linked GlcNAc transferase encoded by a single mammalian gene. *Arch. Biochem. Biophys.* **409**, 287–297
 28. Nolte, D., and Müller, U. (2002) Human O-GlcNAc transferase (OGT): genomic structure, analysis of splice variants, fine mapping in Xq13.1. *Mamm. Genome* **13**, 62–64
 29. Hanover, J. A., Forsythe, M. E., Hennessey, P. T., Brodigan, T. M., Love, D. C., Ashwell, G., and Krause, M. (2005) A *Caenorhabditis elegans* model of insulin resistance: altered macronutrient storage and dauer formation in an OGT-1 knockout. *Proc. Natl. Acad. Sci. U.S.A.* **102**, 11266–11271
 30. Gambetta, M. C., Oktaba, K., and Müller, J. (2009) Essential role of the glycosyltransferase *scx*/*Ogt* in Polycomb repression. *Science* **325**, 93–96
 31. Sinclair, D. A., Syrzycka, M., Macauley, M. S., Rastgardani, T., Komljenovic, I., Voadlo, D. J., Brock, H. W., and Honda, B. M. (2009) *Drosophila* O-GlcNAc transferase (OGT) is encoded by the Polycomb group (PcG) gene, super sex combs (*scx*). *Proc. Natl. Acad. Sci. U.S.A.* **106**, 13427–13432
 32. Sohn, K. C., and Do, S. I. (2005) Transcriptional regulation and O-GlcNAcylation activity of zebrafish OGT during embryogenesis. *Biochem. Biophys. Res. Commun.* **337**, 256–263
 33. Comtesse, N., Maldener, E., and Meese, E. (2001) Identification of a nuclear variant of MGEA5, a cytoplasmic hyaluronidase and a β -*N*-acetylglucosaminidase. *Biochem. Biophys. Res. Commun.* **283**, 634–640
 34. Keembiyehetty, C. N., Krzeslak, A., Love, D. C., and Hanover, J. A. (2011) A lipid-droplet-targeted O-GlcNAcase isoform is a key regulator of the proteasome. *J. Cell Sci.* **124**, 2851–2860
 35. Forsythe, M. E., Love, D. C., Lazarus, B. D., Kim, E. J., Prinz, W. A., Ashwell, G., Krause, M. W., and Hanover, J. A. (2006) *Caenorhabditis elegans* ortholog of a diabetes susceptibility locus: *oga-1* (O-GlcNAcase) knockout impacts O-GlcNAc cycling, metabolism, and dauer. *Proc. Natl. Acad. Sci. U.S.A.* **103**, 11952–11957
 36. Toleman, C., Paterson, A. J., Whisenhunt, T. R., and Kudlow, J. E. (2004) Characterization of the histone acetyltransferase (HAT) domain of a bifunctional protein with activable O-GlcNAcase and HAT activities. *J. Biol. Chem.* **279**, 53665–53673
 37. Butkinaree, C., Cheung, W. D., Park, S., Park, K., Barber, M., and Hart, G. W. (2008) Characterization of β -*N*-acetylglucosaminidase cleavage by caspase-3 during apoptosis. *J. Biol. Chem.* **283**, 23557–23566
 38. Rao, F. V., Schüttelkopf, A. W., Dorfmueller, H. C., Ferenbach, A. T., Navratilova, I., and van Aalten, D. M. (2013) Structure of a bacterial putative acetyltransferase defines the fold of the human O-GlcNAcase C-terminal domain. *Open Biol.* **3**, 130021
 39. He, Y., Roth, C., Turkenburg, J. P., and Davies, G. J. (2014) Three-dimensional structure of a *Streptomyces sviveus* GNAT acetyltransferase with similarity to the C-terminal domain of the human GH84 O-GlcNAcase. *Acta Crystallogr. D Biol. Crystallogr.* **70**, 186–195
 40. Shafi, R., Iyer, S. P., Ellies, L. G., O'Donnell, N., Marek, K. W., Chui, D., Hart, G. W., and Marth, J. D. (2000) The O-GlcNAc transferase gene resides on the X chromosome and is essential for embryonic stem cell viability and mouse ontogeny. *Proc. Natl. Acad. Sci. U.S.A.* **97**, 5735–5739
 41. Yang, Y. R., Song, M., Lee, H., Jeon, Y., Choi, E. J., Jang, H. J., Moon, H. Y., Byun, H. Y., Kim, E. K., Kim, D. H., Lee, M. N., Koh, A., Ghim, J., Choi, J. H., Lee-Kwon, W., Kim, K. T., Ryu, S. H., and Suh, P. G. (2012) O-GlcNAcase is essential for embryonic development and maintenance of genomic stability. *Aging Cell* **11**, 439–448
 42. Webster, D. M., Teo, C. F., Sun, Y., Wloga, D., Gay, S., Klonowski, K. D., Wells, L., and Dougan, S. T. (2009) O-GlcNAc modifications regulate cell survival and epiboly during zebrafish development. *BMC Dev. Biol.* **9**, 28
 43. Dehennaut, V., Hanouille, X., Bodart, J. F., Vilain, J. P., Michalski, J. C., Landrieu, I., Lippens, G., and Lefebvre, T. (2008) Microinjection of recombinant O-GlcNAc transferase potentiates *Xenopus* oocytes M-phase entry. *Biochem. Biophys. Res. Commun.* **369**, 539–546
 44. Rahman, M. M., Stuchlick, O., El-Karim, E. G., Stuart, R., Kipreos, E. T., and Wells, L. (2010) Intracellular protein glycosylation modulates insulin mediated lifespan in *C. elegans*. *Aging* **2**, 678–690
 45. Wang, P., Lazarus, B. D., Forsythe, M. E., Love, D. C., Krause, M. W., and Hanover, J. A. (2012) O-GlcNAc cycling mutants modulate proteotoxicity in *Caenorhabditis elegans* models of human neurodegenerative diseases. *Proc. Natl. Acad. Sci. U.S.A.* **109**, 17669–17674
 46. Wang, P., and Hanover, J. A. (2013) Nutrient-driven O-GlcNAc cycling influences autophagic flux and neurodegenerative proteotoxicity. *Autophagy* **9**, 604–606
 47. van den Ent, F., and Löwe, J. (2006) RF cloning: a restriction-free method for inserting target genes into plasmids. *J. Biochem. Biophys. Methods* **67**, 67–74
 48. Borodkin, V. S., Schimpl, M., Gundogdu, M., Rafie, K., Dorfmueller, H. C., Robinson, D. A., and van Aalten, D. M. (2014) Bisubstrate UDP-peptide conjugates as human O-GlcNAc transferase inhibitors. *Biochem. J.* **457**, 497–502
 49. Lee, H. S., and Thorson, J. S. (2011) Development of a universal glycosyltransferase assay amenable to high-throughput formats. *Anal. Biochem.* **418**, 85–88
 50. Ojida, A., Takashima, I., Kohira, T., Nonaka, H., and Hamachi, I. (2008) Turn-on fluorescence sensing of nucleoside polyphosphates using a xanthene-based Zn(II) complex chemosensor. *J. Am. Chem. Soc.* **130**, 12095–12101
 51. Rao, F. V., Dorfmueller, H. C., Villa, F., Allwood, M., Eggleston, I. M., and van Aalten, D. M. (2006) Structural insights into the mechanism and inhibition of eukaryotic O-GlcNAc hydrolysis. *EMBO J.* **25**, 1569–1578
 52. Schimpl, M., Zheng, X., Borodkin, V. S., Blair, D. E., Ferenbach, A. T., Schüttelkopf, A. W., Navratilova, I., Aristotelous, T., Albarbarawi, O., Robinson, D. A., Macnaughtan, M. A., and van Aalten, D. M. (2012) O-GlcNAc transferase invokes nucleotide sugar pyrophosphate participation in catalysis. *Nat. Chem. Biol.* **8**, 969–974
 53. Jakob, W., Sagasser, S., Dellaporta, S., Holland, P., Kuhn, K., and Schierwater, B. (2004) The *Trox-2* Hox/ParaHox gene of *Trichoplax* (Placozoa) marks an epithelial boundary. *Dev. Genes Evol.* **214**, 170–175
 54. Machida, M., and Jigami, Y. (1994) Glycosylated DNA-binding proteins from filamentous fungus, *Aspergillus oryzae*: modification with *N*-acetylglucosamine monosaccharide through an O-glycosidic linkage. *Biosci. Biotech. Biochem.* **58**, 344–348
 55. Perez-Cervera, Y., Harichaux, G., Schmidt, J., Debierre-Grockiego, F., Dehennaut, V., Bieker, U., Meurice, E., Lefebvre, T., and Schwarz, R. T. (2011) Direct evidence of O-GlcNAcylation in the apicomplexan *Toxoplasma gondii*: a biochemical and bioinformatic study. *Amino Acids* **40**, 847–856
 56. Banerjee, S., Robbins, P. W., and Samuelson, J. (2009) Molecular characterization of nucleocytoplasmic O-GlcNAc transferases of *Giardia lamblia* and *Cryptosporidium parvum*. *Glycobiology* **19**, 331–336
 57. Fredriksen, L., Mathiesen, G., Moen, A., Bron, P. A., Kleerebezem, M., Eijsink, V. G., and Egge-Jacobsen, W. (2012) The major autolysin *AcM2* from *Lactobacillus plantarum* undergoes cytoplasmic O-glycosylation. *J. Bacteriol.* **194**, 325–333
 58. Schirm, M., Kalmokoff, M., Aubry, A., Thibault, P., Sandoz, M., and Logan, S. M. (2004) Flagellin from *Listeria monocytogenes* is glycosylated

- with β -O-linked N-acetylglucosamine. *J. Bacteriol.* **186**, 6721–6727
59. Olszewski, N. E., West, C. M., Sassi, S. O., and Hartweck, L. M. (2010) O-GlcNAc protein modification in plants: evolution and function. *Biochim. Biophys. Acta* **1800**, 49–56
60. Srivastava, M., Begovic, E., Chapman, J., Putnam, N. H., Hellsten, U., Kawashima, T., Kuo, A., Mitros, T., Salamov, A., Carpenter, M. L., Signorovitch, A. Y., Moreno, M. A., Kamm, K., Grimwood, J., Schmutz, J., Shapiro, H., Grigoriev, I. V., Buss, L. W., Schierwater, B., Dellaporta, S. L., and Rokhsar, D. S. (2008) The *Trichoplax* genome and the nature of placozoans. *Nature* **454**, 955–960
61. Schierwater, B. (2005) My favorite animal, *Trichoplax adhaerens*. *BioEssays* **27**, 1294–1302
62. Dellaporta, S. L., Xu, A., Sagasser, S., Jakob, W., Moreno, M. A., Buss, L. W., and Schierwater, B. (2006) Mitochondrial genome of *Trichoplax adhaerens* supports Placozoa as the basal lower metazoan phylum. *Proc. Natl. Acad. Sci. U.S.A.* **103**, 8751–8756
63. Smith, C. L., Varoqueaux, F., Kittelmann, M., Azzam, R. N., Cooper, B., Winters, C. A., Eitel, M., Fasshauer, D., and Reese, T. S. (2014) Novel cell types, neurosecretory cells, and body plan of the early-diverging metazoan *Trichoplax adhaerens*. *Curr. Biol.* **24**, 1565–1572
64. Lubas, W. A., Frank, D. W., Krause, M., and Hanover, J. A. (1997) O-Linked GlcNAc transferase is a conserved nucleocytoplasmic protein containing tetratricopeptide repeats. *J. Biol. Chem.* **272**, 9316–9324
65. Macauley, M. S., Whitworth, G. E., Debowski, A. W., Chin, D., and Vocadlo, D. J. (2005) O-GlcNAcase uses substrate-assisted catalysis: kinetic analysis and development of highly selective mechanism-inspired inhibitors. *J. Biol. Chem.* **280**, 25313–25322
66. Schimpl, M., Schüttelkopf, A. W., Borodkin, V. S., and van Aalten, D. M. (2010) Human OGA binds substrates in a conserved peptide recognition groove. *Biochem. J.* **432**, 1–7
67. Ringrose, J. H., van den Toorn, H. W., Eitel, M., Post, H., Neerinx, P., Schierwater, B., Altelaar, A. F., and Heck, A. J. (2013) Deep proteome profiling of *Trichoplax adhaerens* reveals remarkable features at the origin of metazoan multicellularity. *Nat. Commun.* **4**, 1408
68. Martinelli, C., and Spring, J. (2003) Distinct expression patterns of the two T-box homologues Brachyury and Tbx2/3 in the placozoan *Trichoplax adhaerens*. *Dev. Genes Evol.* **213**, 492–499
69. Martinelli, C., and Spring, J. (2004) Expression pattern of the homeobox gene Not in the basal metazoan *Trichoplax adhaerens*. *Gene Expr. Patterns* **4**, 443–447
70. Hadrys, T., DeSalle, R., Sagasser, S., Fischer, N., and Schierwater, B. (2005) The *Trichoplax PaxB* gene: a putative Proto-PaxA/B/C gene predating the origin of nerve and sensory cells. *Mol. Biol. Evol.* **22**, 1569–1578
71. Kreppel, L. K., Blomberg, M. A., and Hart, G. W. (1997) Dynamic glycosylation of nuclear and cytosolic proteins: cloning and characterization of a unique O-GlcNAc transferase with multiple tetratricopeptide repeats. *J. Biol. Chem.* **272**, 9308–9315
72. Kreppel, L. K., and Hart, G. W. (1999) Regulation of a cytosolic and nuclear O-GlcNAc transferase: role of the tetratricopeptide repeats. *J. Biol. Chem.* **274**, 32015–32022
73. Shen, D. L., Gloster, T. M., Yuzwa, S. A., and Vocadlo, D. J. (2012) Insights into O-linked N-acetylglucosamine ((0–9)O-GlcNAc) processing and dynamics through kinetic analysis of O-GlcNAc transferase and O-GlcNAcase activity on protein substrates. *J. Biol. Chem.* **287**, 15395–15408
74. Lazarus, B. D., Roos, M. D., and Hanover, J. A. (2005) Mutational analysis of the catalytic domain of O-linked N-acetylglucosaminyl transferase. *J. Biol. Chem.* **280**, 35537–35544
75. Lubas, W. A., and Hanover, J. A. (2000) Functional expression of O-linked GlcNAc transferase: domain structure and substrate specificity. *J. Biol. Chem.* **275**, 10983–10988
76. Lazarus, M. B., Nam, Y., Jiang, J., Sliz, P., and Walker, S. (2011) Structure of human O-GlcNAc transferase and its complex with a peptide substrate. *Nature* **469**, 564–567
77. Tarrant, M. K., Rho, H. S., Xie, Z., Jiang, Y. L., Gross, C., Culhane, J. C., Yan, G., Qian, J., Ichikawa, Y., Matsuoka, T., Zachara, N., Etzkorn, F. A., Hart, G. W., Jeong, J. S., Blackshaw, S., Zhu, H., and Cole, P. A. (2012) Regulation of CK2 by phosphorylation and O-GlcNAcylation revealed by semisynthesis. *Nat. Chem. Biol.* **8**, 262–269
78. Kim, E. J., Kang, D. O., Love, D. C., and Hanover, J. A. (2006) Enzymatic characterization of O-GlcNAcase isoforms using a fluorogenic GlcNAc substrate. *Carbohydr. Res.* **341**, 971–982
79. Macauley, M. S., and Vocadlo, D. J. (2009) Enzymatic characterization and inhibition of the nuclear variant of human O-GlcNAcase. *Carbohydr. Res.* **344**, 1079–1084
80. Dorfmueller, H. C., Borodkin, V. S., Schimpl, M., Shepherd, S. M., Shpiro, N. A., van and Aalten, D. M. (2006) GlcNAcstatin: a picomolar, selective O-GlcNAcase inhibitor that modulates intracellular O-GlcNAcylation levels. *J. Am. Chem. Soc.* **128**, 16484–16485
81. Dorfmueller, H. C., Borodkin, V. S., Schimpl, M., and van Aalten, D. M. (2009) GlcNAcstatins are nanomolar inhibitors of human O-GlcNAcase inducing cellular hyper-O-GlcNAcylation. *Biochem. J.* **420**, 221–227
82. Yuzwa, S. A., Macauley, M. S., Heinonen, J. E., Shan, X., Dennis, R. J., He, Y., Whitworth, G. E., Stubbs, K. A., McEachern, E. J., Davies, G. J., and Vocadlo, D. J. (2008) A potent mechanism-inspired O-GlcNAcase inhibitor that blocks phosphorylation of tau *in vivo*. *Nat. Chem. Biol.* **4**, 483–490
83. Ramakrishnan, B., and Qasba, P. K. (2002) Structure-based design of β 1,4-galactosyltransferase I (β 4Gal-T1) with equally efficient N-acetylgalactosaminyltransferase activity: point mutation broadens β 4Gal-T1 donor specificity. *J. Biol. Chem.* **277**, 20833–20839
84. Khidekel, N., Arndt, S., Lamarre-Vincent, N., Lippert, A., Poulin-Kerstien, K. G., Ramakrishnan, B., Qasba, P. K., and Hsieh-Wilson, L. C. (2003) A chemoenzymatic approach toward the rapid and sensitive detection of O-GlcNAc posttranslational modifications. *J. Am. Chem. Soc.* **125**, 16162–16163
85. Dorfmueller, H. C., and van Aalten, D. M. (2010) Screening-based discovery of drug-like O-GlcNAcase inhibitor scaffolds. *FEBS Lett.* **584**, 694–700
86. Loenarz, C., Coleman, M. L., Boleining, A., Schierwater, B., Holland, P. W., Ratcliffe, P. J., and Schofield, C. J. (2011) The hypoxia-inducible transcription factor pathway regulates oxygen sensing in the simplest animal, *Trichoplax adhaerens*. *EMBO Rep.* **12**, 63–70
87. von der Chevallerie, K., Rolfes, S., and Schierwater, B. (2014) Inhibitors of the p53-Mdm2 interaction increase programmed cell death and produce abnormal phenotypes in the placozoan *Trichoplax adhaerens* (F.E. Schulze). *Dev. Genes Evol.* **224**, 79–85
88. Frédéric, M. Y., Lundin, V. F., Whiteside, M. D., Cueva, J. G., Tu, D. K., Kang, S. Y., Singh, H., Baillie, D. L., Hutter, H., Goodman, M. B., Brinkman, F. S., and Leroux, M. R. (2013) Identification of 526 conserved metazoan genetic innovations exposes a new role for cofactor E-like in neuronal microtubule homeostasis. *PLoS Genet.* **9**, e1003804
89. Lim, W. A., and Pawson, T. (2010) Phosphotyrosine signaling: evolving a new cellular communication system. *Cell* **142**, 661–667

**Glycobiology and Extracellular Matrices:
The Early Metazoan *Trichoplax adhaerens*
Possesses a Functional *O*-GlcNAc System**



Nithya Selvan, Daniel Mariappa, Henk W. P.
van den Toorn, Albert J. R. Heck, Andrew T.
Ferenbach and Daan M. F. van Aalten

J. Biol. Chem. 2015, 290:11969-11982.

doi: 10.1074/jbc.M114.628750 originally published online March 16, 2015

Access the most updated version of this article at doi: [10.1074/jbc.M114.628750](https://doi.org/10.1074/jbc.M114.628750)

Find articles, minireviews, Reflections and Classics on similar topics on the [JBC Affinity Sites](#).

Alerts:

- [When this article is cited](#)
- [When a correction for this article is posted](#)

[Click here](#) to choose from all of JBC's e-mail alerts

Supplemental material:

<http://www.jbc.org/content/suppl/2015/03/16/M114.628750.DC1.html>

This article cites 89 references, 45 of which can be accessed free at
<http://www.jbc.org/content/290/19/11969.full.html#ref-list-1>